

# Determination of masses and radii of the massive eclipsing binary system HV 2543 in the Large Magellanic Cloud

P.G. Ostrov<sup>1,\*</sup>, E. Lapasset<sup>2,3</sup>, and N.I. Morrell<sup>1,3</sup>

<sup>1</sup> Facultad de Ciencias Astronómicas y Geofísicas, Universidad Nacional de La Plata, Paseo del Bosque S/N, 1900 La Plata, Argentina

<sup>2</sup> Observatorio Astronómico, Universidad Nacional de Córdoba, Laprida 854, 5000 Córdoba, Argentina

<sup>3</sup> Member of the Carrera del Investigador Científico, CONICET, Argentina

Received 5 November 1999 / Accepted 14 February 2000

**Abstract.** We present a  $V$  light curve of the eclipsing binary system HV 2543 (Sk-67°117) in the Large Magellanic Cloud based on CCD images acquired between the years 1995 and 1998. We have analysed this light curve and published radial velocity data, finding that this system is semidetached, with the secondary (less massive and less luminous component) filling its Roche lobe. From our analysis with the Wilson-Devinney code, we estimated the following masses and radii for the components of HV 2543:  $M_1 = 25.63 \pm 0.7 M_\odot$ ,  $R_1 = 15.54 \pm 0.4 R_\odot$ ,  $M_2 = 15.63 \pm 1.0 M_\odot$  and  $R_2 = 13.99 \pm 0.4 R_\odot$ . On the basis of  $B$  and  $V$  photometry of the field stars, we found that HV 2543 is member of an OB association, perhaps related to which the massive binary system Sk-67°105 belongs.

**Key words:** stars: binaries: eclipsing – stars: fundamental parameters – stars: early-type – stars: individual: HV 2543

## 1. Introduction

The analysis of light curves of eclipsing binaries, in addition to radial velocity data, provides fundamental knowledge about the masses and physical dimensions of the stars. Studying massive binaries in the Magellanic Clouds we can learn about the evolution of these systems at metallicities lower than that of our galaxy.

The Harvard variable HV 2543 ( $\alpha = 5^{\text{h}}27^{\text{m}}27^{\text{s}}$ ,  $\delta = -67^\circ 11'54''$ , J2000) is a hot binary star in the LMC. It was catalogued as an OB star by Sanduleak (1969), who assigned it the identification -67°117. The eclipsing nature of this binary was discovered by Gaposhkin (1970), who published a photographic light curve fitting a period of 4.829052 days (see also Payne-Gaposhkin 1971). Photoelectric photometry was performed by Isserstedt (1979) who found  $V = 12.92$ ,  $(B - V) = -0.18$  and  $(U - B) = -1.03$ . Radial velocity orbit was obtained by

*Send offprint requests to:* P.G. Ostrov

\* Visiting Astronomer, Complejo Astronómico El Leoncito operated under agreement between the Consejo Nacional de Investigaciones Científicas y Técnicas de la República Argentina and the National Universities of La Plata, Córdoba and San Juan.

*Correspondence to:* ostrov@fcaglp.edu.ar

**Table 1.** Instrumental configuration

Detector	Tektronix 1024 × 1024 CCD
readout noise	10.4 e <sup>-</sup>
gain	7.97 e <sup>-</sup> /ADU
filters	Johnson $V$ and $B$
telescope configuration	direct CCD + focal reducer
focal relation	2.83
scale	0.813 arcsec pixel <sup>-1</sup>
field size	diameter $\sim 9'$ , circular

Niemela & Bassino (1994) who derived physical parameters of the binary components and concluded that HV 2543 was a semidetached system with the less massive component filling its equipotential Roche surface. On the basis of their spectroscopic data, they classified this system as O8V:+O9III. Smith Neubig & Bruhweiler (1999) have published an UV spectral classification of LMC OB stars based on IUE data, assigning to HV 2543 the type O9III.

In this paper we present a CCD  $V$  light curve for HV 2543. By means of the combined analysis of these data and previously published radial velocities, we derive new values of the fundamental parameters of this system.

The paper is organized as follows: in Sect. 2 we describe the observations, reductions and calibration steps. In Sect. 3 we describe the photometric results and light curve fitting. In Sect. 4 we discuss the results and in Sect. 5 we present our conclusions.

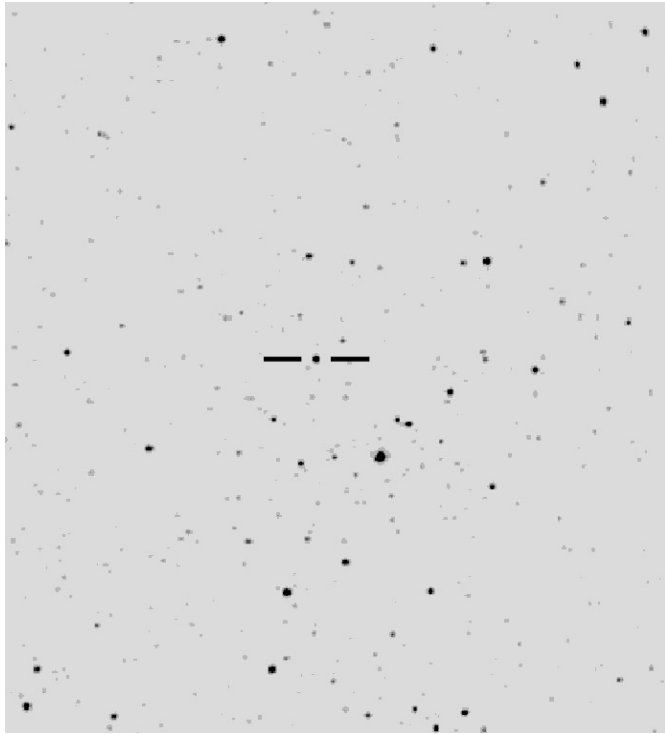
## 2. Data acquisition and reductions

### 2.1. Observations

The CCD images here analysed were acquired with the 2.15-m telescope at CASLEO, during three runs in 1995, 1997 and 1998. About five frames of the HV 2543 field were obtained each night, except during eclipses, when the observation was more intensive. During each observing night, a series of 10  $\sim$  15 twilight flats and bias frames was also obtained. In addition, for the 1997 and 1998 runs, 10  $\sim$  15 dome flats were also obtained each night. Tables 1 and 2 list details of the observations and Fig. 1 shows a finding chart for HV 2543.

**Table 2.** Observing logs

date	1995, Oct 21–25	1997, Nov 15–21	1998, Dec 2–8
HJD-2450000	0011–0016	0767–0774	1149–1156
number of images acquired $\times$ filter	$35 \times V$	$19 \times B + 42 \times V$	$36 \times V$
range of exp. times [s]	15–40	5–40	7–30

**Fig. 1.** Finding chart for HV 2543. North is at the top and East is at the left. The size of the region displayed is approximately  $5.4' \times 6.4'$ 

## 2.2. Reductions and photometry

Reductions were performed using IRAF routines. For each night, the frames were reduced in the standard way (overscan and bias corrections, flat fielding) using properly combined bias and flat frames. The illumination differences between sky-flats and dome-flats were found to be less than 0.3% at the edges of the frames, and negligible at the center. Whenever high quality sky-flats (that is, zero clouds) were available, these were preferred to dome-flats.

For each observing run, the following steps were performed:

1. A master image was made by aligning and combining the highest quality frames (best seeing and darkest sky). On this combined image, a profile fitting photometry was performed using a stand-alone version of DAOPHOT II (Stetson 1987, Stetson 1991). The resulting output was used as master coordinate list in the following steps.
2. Aperture photometry was performed on each individual frame using a circular diaphragm of  $9.5''$  diameter. The sky background was determined locally for each star using a sky annulus of radii  $9.76$  and  $20.33''$ .

3. A list of instrumental magnitudes for each individual frame and for each star in the master list was constructed.

Five faint neighbour stars were detected in the combined frame within a radius of  $9''$  around HV 2543, being the brightest of these some 5 mag fainter than the binary. Light contamination from these stars slightly contributes to the measured magnitude of HV 2543 (differences of the order of 0.014 mag). Consequently, an adequate flux correction was applied to the aperture photometry.

## 2.3. Photometric calibration

No single objects were chosen as comparison and check stars. Instead, zero point corrections were computed for each frame using a group of  $\sim 15$  stars, covering widely the range of magnitudes of HV 2543. To put all the observations in a unique instrumental system, we proceeded as follows:

1. A synthetic reference system was defined using the mean instrumental magnitudes of the calibration stars.
2. For each frame, a zero point offset was computed and the magnitudes were transformed to the synthetic reference system.
3. After this transformation, the RMS residuals were computed for each star. Only the stars with the smallest residuals ( $< 0.01$ ) were conserved as calibration stars.
4. We repeated these steps with the new, cleaned calibration star list.

Since all nights were not really photometric, this procedure allowed us to have a direct estimate of the internal errors of each image.

The above enumerated steps were performed independently for each observing run. We proceeded in this way because the stars available as calibrators are not the same for each run, due to pointing differences. On the other hand, some stars remain perfectly stable during a run, but show luminosity variations from one year to another, being then inadequate as calibrators between different runs.

After this first stage of calibration was complete, a list of robust estimates of instrumental stellar magnitudes and their dispersions was constructed for each run. After cross identification between the three lists, the most stable stars were selected to serve as calibrators between the different runs.

During the 1997 run, 19 frames through the Johnson's  $B$  band were also acquired. These frames were used to determine the transformations to the standard  $V$  system.

The final transformations to the standard system were performed by means of aperture photometry of 33 standard stars –

ranging from  $(B - V) = -.004$  to  $2.192$  – from Landolt (1992) acquired during the photometric nights.

We used the following transformation equations:

$$b = B + b_1 + b_2 X + b_3 (B - V)$$

$$v = V + v_1 + v_2 X + v_3 (B - V)$$

We adopted the mean values of the extinction coefficients given by Minniti et al. (1989) and obtained the following values for the other coefficients:

Nov. 19, 1997:

$$b_1 = 4.2826 \pm 0.0105$$

$$b_3 = -0.0208 \pm 0.0115$$

$$v_1 = 3.4446 \pm 0.0051$$

$$v_3 = -0.0456 \pm 0.0055$$

Nov. 20, 1997:

$$b_1 = 4.2986 \pm 0.0076$$

$$b_3 = -0.03116 \pm 0.0086$$

$$v_1 = 3.4502 \pm 0.0057$$

$$v_3 = -0.0535 \pm 0.0067$$

The RMS residuals of the  $V$  transformations were  $0.017$  mag. We first shifted our unified instrumental system to that corresponding to a  $V$  frame acquired immediately before a series of  $B$  exposures, on Nov. 19, 1997. Then, we applied the standard transformations derived for that night. The Nov. 20 transformations were used only to check the quality of the first ones.

Our photometry of HV 2543 is presented in Table 3. In successive columns the heliocentric julian day, standard  $V$  magnitude, internal errors, seeing and airmass are given. The errors ( $\sigma_i$ ) account for the internal photometric errors estimated by DAOPHOT and those of the transformation to an unified instrumental system. They do not include the error of the transformation to the standard system.

### 3. Results

#### 3.1. Ephemeris

We have observed one primary minimum during 1997, at HJD =  $2\,450\,768^{\text{d}}.802 \pm 0.001$ . Combining this value with that given by Payne-Gaposchkin (1971) we obtained a new ephemerides for HV 2543:

$$E_0 = 2\,450\,768^{\text{d}}.802 \pm 0.001$$

$$P = 4^{\text{d}}.829\,046 \pm 0.000\,004$$

We have used this ephemeris in calculating the phases for the radial velocity and photometric data.

#### 3.2. Light and radial velocity curve analysis

The  $V$  light curve of HV 2543 is typical of near-contact binaries, with different depths of the minima and continuous variations of

light in out-of-eclipse portions. Also noticeable is the O'Connell effect, i.e., the small difference in magnitude between both maxima (see Davidge & Milone 1984). We solved simultaneously the light and radial velocity curves using the Wilson & Devinney code (hereafter WD), which is very well suited for the study of close binary systems (Wilson & Devinney 1971, Wilson 1990). Unit weight was given to photometric CCD observations since they all were collected with the same instrumental configuration and have comparable quality. A unit weight was also given to most of the radial velocity points except for those near eclipses or indicated by Niemela & Bassino (1994) as less confident. We also corrected the data points corresponding to the phase  $\phi = 0.05$ , that are inverted (i.e., the O8 velocity corresponds to the O9 and vice-versa) in Niemela & Bassino (1994). The relation between photometric and spectroscopic weights was given through the values of the mean standard deviations (sigma) of the data which were estimated to be  $17$  and  $12 \text{ km s}^{-1}$  for the radial velocities of the primary and secondary components, respectively, and  $0.02$  mag for the light points. Only the ratios between these values are significant.

The radii that result from our preliminary light curve analysis indicate that the O8 component is more alike an O8III star. Chlebowski & Garmany (1991) give a temperature of  $36000 \text{ K}$  for an O8III star. Given that Schmidt-Kaler (1982) gives a lower temperature for such spectral type, we also performed an analysis assigning a  $34700 \text{ K}$  temperature for the primary. Standard values of bolometric albedos,  $A = 1.0$  (Rucinski 1969), and gravity darkening coefficients,  $g = 1.0$  (Lucy 1976), for radiative envelopes were used. Linear limb-darkening coefficients were determined from tables by van Hamme (1993). These parameters were not adjusted. The adjustable parameters in our computations were:  $a$  (semimajor axis),  $V_\gamma$  (systemic radial velocity),  $i$  (orbital inclination),  $T_2$  (temperature of the secondary component),  $q$  (mass-ratio),  $\Omega_1$  and  $\Omega_2$  (modified potential of both components) and  $L_1$  (luminosity of the primary). The first approaches to fit the observations were made by means of the light curve (LC) program until an acceptable fit to the  $V$  light curve was obtained.

Then we proceeded with the differential corrections (DC) code. We first adjusted the parameters  $a$ ,  $V_\gamma$  and  $q$  using only the out-of-eclipses radial velocity data. Thereupon, we left those parameters fixed and fitted  $i$ ,  $T_2$ ,  $\Omega_1$ ,  $\Omega_2$  and  $L_1$ , using only the light curve. Then we re-computed the first set of parameters leaving fixed the second set, and iterated this procedure until the corrections were smaller than their errors. A better solution was achieved allowing the fit of  $q$  with the photometric data, that is, including  $q$  within the second parameter set. Mode 2 (Leung & Wilson 1977) which stands for detached systems was used at the beginning, but after a few runs of the DC program the computations clearly evolved towards a semidetached configuration with the secondary component filling its critical Roche lobe. Thus, mode 5 of the WD code was employed until the final solutions were found. In this mode, the parameter  $\Omega_2$  cannot be adjusted and it is set equal to the critical filling-lobe value. The solutions never converged to contact configurations.

**Table 3.** *V* light photometry of HV 2543.

HJD	<i>V</i>	$\sigma_i$	fwhm	<i>X</i>	HJD	<i>V</i>	$\sigma_i$	fwhm	<i>X</i>
2450000+			"		2450000+			"	
11.680	12.807	0.009	2.98	1.51	771.812	12.919	0.005	2.56	1.26
11.726	12.803	0.013	2.34	1.36	771.850	12.905	0.006	2.61	1.31
11.768	12.806	0.013	2.44	1.26	772.637	12.872	0.006	2.66	1.37
11.812	12.790	0.012	3.31	1.23	772.681	12.872	0.008	2.84	1.28
12.668	12.988	0.010	3.03	1.54	772.753	12.881	0.006	2.61	1.23
12.730	13.032	0.010	3.98	1.34	772.806	12.884	0.006	2.78	1.25
12.768	13.074	0.009	3.94	1.27	772.856	12.887	0.007	3.04	1.33
12.810	13.119	0.010	4.15	1.23	773.593	13.759	0.006	2.43	1.51
12.838	13.156	0.013	4.67	1.23	773.658	13.763	0.007	2.00	1.32
12.864	13.204	0.016	4.71	1.23	773.708	13.674	0.004	2.41	1.25
13.683	12.912	0.010	2.88	1.47	773.729	13.629	0.004	2.51	1.23
13.732	12.900	0.010	3.30	1.33	773.742	13.609	0.005	2.42	1.23
13.773	12.883	0.013	3.76	1.26	773.754	13.572	0.005	3.24	1.23
13.852	12.865	0.009	3.14	1.23	773.770	13.540	0.006	2.61	1.23
14.665	12.879	0.006	3.38	1.53	773.780	13.506	0.005	2.69	1.23
14.718	12.894	0.006	4.07	1.36	773.791	13.479	0.007	3.11	1.24
14.755	12.903	0.005	3.76	1.28	773.804	13.457	0.008	3.57	1.25
14.791	12.919	0.007	3.94	1.24	773.816	13.414	0.005	2.63	1.27
14.861	12.940	0.015	5.19	1.24	773.833	13.380	0.007	2.60	1.29
15.577	13.607	0.014	4.04	2.07	773.853	13.345	0.011	3.46	1.33
15.584	13.588	0.011	3.24	2.01	1149.809	12.996	0.016	2.19	1.30
15.590	13.570	0.011	3.08	1.96	1149.837	13.020	0.005	2.36	1.36
15.595	13.557	0.010	3.10	1.92	1150.848	12.922	0.012	2.09	1.40
15.603	13.535	0.009	2.75	1.86	1151.616	12.810	0.007	2.27	1.34
15.609	13.523	0.010	3.16	1.82	1151.670	12.814	0.005	2.23	1.25
15.618	13.496	0.009	3.67	1.76	1151.730	12.820	0.004	2.05	1.23
15.628	13.462	0.010	3.48	1.70	1151.785	12.825	0.007	2.48	1.27
15.643	13.432	0.009	3.32	1.62	1151.853	12.838	0.007	2.20	1.42
15.675	13.361	0.010	2.34	1.48	1152.644	13.386	0.006	2.57	1.28
15.693	13.305	0.011	2.79	1.42	1152.662	13.414	0.006	2.54	1.25
15.717	13.265	0.010	3.20	1.35	1152.690	13.443	0.006	1.93	1.23
15.738	13.220	0.012	3.81	1.31	1152.708	13.454	0.005	2.18	1.23
15.787	13.151	0.010	3.73	1.24	1152.728	13.457	0.004	2.42	1.23
15.834	13.077	0.011	4.11	1.23	1152.737	13.456	0.005	2.19	1.23
15.865	13.048	0.010	3.32	1.24	1152.750	13.447	0.006	2.10	1.24
767.694	12.848	0.009	2.35	1.28	1152.761	13.434	0.005	1.97	1.25
767.768	12.857	0.006	3.05	1.23	1152.786	13.401	0.004	2.21	1.28
767.808	12.864	0.008	3.68	1.24	1152.799	13.384	0.007	2.14	1.30
767.849	12.866	0.005	3.09	1.29	1152.812	13.358	0.003	1.84	1.32
768.627	13.451	0.009	3.11	1.44	1152.829	13.335	0.004	2.01	1.36
768.685	13.607	0.007	2.77	1.29	1152.855	13.295	0.008	2.35	1.44
768.748	13.743	0.007	2.32	1.23	1153.687	12.842	0.008	1.57	1.23
768.803	13.790	0.006	2.38	1.24	1153.733	12.833	0.005	1.79	1.23
768.825	13.786	0.006	2.30	1.26	1153.766	12.832	0.007	2.05	1.25
768.840	13.758	0.006	2.32	1.28	1153.821	12.828	0.006	2.24	1.35
768.856	13.738	0.008	2.17	1.31	1153.857	12.825	0.006	2.86	1.45
768.868	13.718	0.015	2.19	1.33	1154.704	13.044	0.007	2.15	1.23
769.639	12.871	0.007	2.93	1.39	1154.738	13.082	0.007	2.80	1.23
769.716	12.860	0.015	3.01	1.25	1154.797	13.151	0.009	2.50	1.30
769.792	12.847	0.011	3.37	1.23	1154.843	13.228	0.005	2.36	1.42
769.835	12.836	0.006	2.86	1.28	1155.656	12.962	0.007	2.16	1.25
770.718	12.937	0.009	1.96	1.24	1155.710	12.935	0.005	1.94	1.23
770.766	12.963	0.006	2.39	1.23	1155.746	12.923	0.006	1.86	1.24
770.814	12.990	0.005	2.21	1.25	1155.774	12.907	0.006	1.82	1.27
770.845	13.020	0.005	1.78	1.30	1155.823	12.886	0.007	2.64	1.37
771.701	12.951	0.012	2.27	1.26	1155.849	12.883	0.005	2.66	1.44
771.777	12.923	0.011	2.47	1.23					

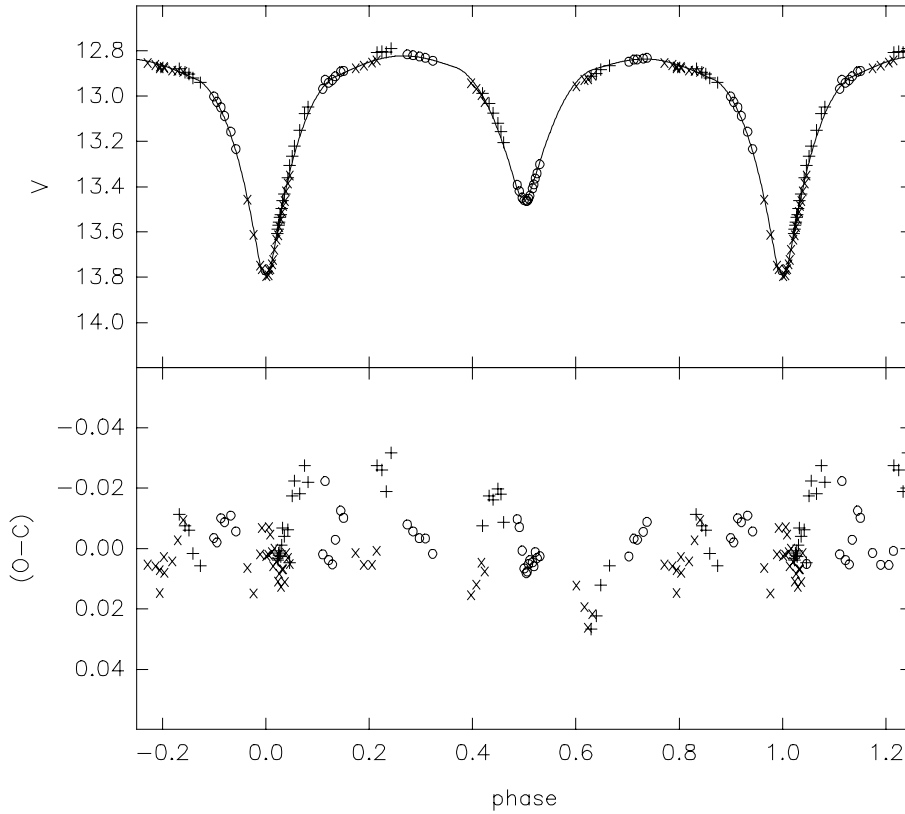


**Fig. 2.** Top: Observed and modelled light curve for HV 2543. Bottom: (O-C) residuals for the light curve. The symbols +, × and ○ correspond to the data collected during 1995, 1997 and 1998 respectively.

Since some systematic differences were obtained between the observed and modelled light curves (due to the O’Connell effect), we tried to improve the binary modelling by including one or two hot spots on the surface of the stars. The spots were placed at the equator of the stars (colatitude = 90°) while the other spot parameters were adjusted with the WD code. The range of the adjusted temperature for the secondary star,  $T_2$ , depends on the adopted value for  $T_1$ . To estimate the errors of the other parameters we considered the differences between the values that arised from different solutions (i.e., using the “spectroscopic” value of  $q$ , 0.55, or leaving it to increase until 0.64, to allow a better fit to the photometric data). The adopted solution, with  $q = 0.61$ , is a compromise between the optimal fit of the light curve and the tolerable deviation from the spectroscopic data. Table 4, lists the model parameters. Figs. 2 and 3 show the modelled light and radial velocity curves, respectively, derived from the one spot solution and plotted along with the observations, and their corresponding residuals (O-C).

The final value of the orbital inclination is incidentally high, very close to 90°. This fact should produce a total eclipse at the secondary minimum, but, as the dimensions of both components are quite similar, this is not a noticeable feature of the observed light curve.

Absolute values of the masses, dimensions and bolometric magnitudes of HV 2543 were computed from the one spot solution. They are listed in Table 5 where  $R_1$  and  $R_2$  correspond to mean values of the derived polar, back and side radii of the stars. The final configuration of HV 2543 shows two components of

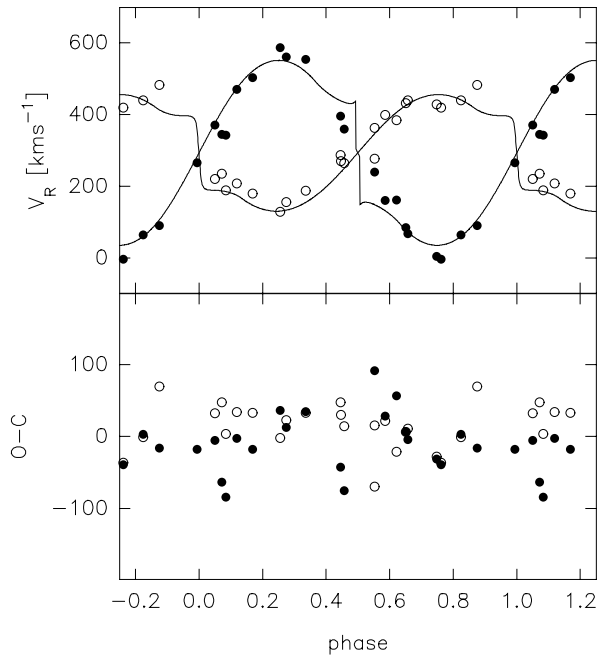


**Fig. 3.** Top: Observed and modelled radial velocity curve for HV 2543. Bottom: (O-C) residuals for the radial velocities. Hollow circles correspond to the primary component and filled ones stand for the secondary.

similar dimensions but different masses and temperatures, with the secondary less massive star filling its Roche lobe.

**Table 4.** Model Parameters

$a$	$41.5 \pm 0.5 R_{\odot}$
$V_{\gamma}$	$293.2 \pm 6 \text{ kms}^{-1}$
$i$	$89 \pm 1^{\circ}$
$q (M_2/M_1)$	$0.61 \pm 0.05$
$T_1$	$36000 \sim 34700 \text{ K}$ (adopted)
$\Omega_1$	$3.363 \pm 0.06$
$g_1$	1.00 (adopted)
$A_1$	1.00 (adopted)
$x_1^b$	0.541 (adopted)
$T_2$	$29200 \sim 28180 \text{ K}^a$
$\Omega_2$	$3.082 \pm 0.12$
$g_2$	1.00 (adopted)
$A_2$	1.00 (adopted)
$x_2^b$	0.561 (adopted)

One hot spot solution (in star 1):

colatitude	$90^{\circ}$
longitude	$253.4^{\circ}$
angular radius	$35.8^{\circ}$
temp. factor	1.053

Two hot spot solution:

For star 1:

colatitude	$90^{\circ}$
longitude	$270^{\circ}$
angular radius	$39.1^{\circ}$
temp. factor	1.032

For star 2:

colatitude	$90^{\circ}$
longitude	$0^{\circ}$
angular radius	$80^{\circ}$
temp. factor	1.030

<sup>a</sup> Values for  $T_2$  resulting for the above quoted values adopted for  $T_1$  respectively.

<sup>b</sup>  $x_1$  and  $x_2$  stand for the bolometric limb-darkening coefficients.

**Table 5.** Star dimensions

$M_1$	$25.63 \pm 0.7 M_{\odot}$
$R_1$	$15.54 \pm 0.4 R_{\odot}$
$M_{bol 1}$	$-9.12 \sim -8.90^a$
$\log g_1 [cgs]$	$3.46 \pm 0.04$
$M_2$	$15.63 \pm 1.0 M_{\odot}$
$R_2$	$13.99 \pm 0.4 R_{\odot}$
$M_{bol 2}$	$-7.98 \sim -7.82^a$
$\log g_2 [cgs]$	$3.34 \pm 0.01$

<sup>a</sup> The range in the derived bolometric magnitudes corresponds to the range in the values adopted for  $T_1$ .

### 3.3. BV Field photometry

We combined the  $B$  frames acquired during 1997 to make a master  $B$  image, on which we performed a profile fitting photometry. We used this photometry together with that performed on the  $V$  master frame to generate a colour-magnitude diagram, which is shown in Fig. 4.

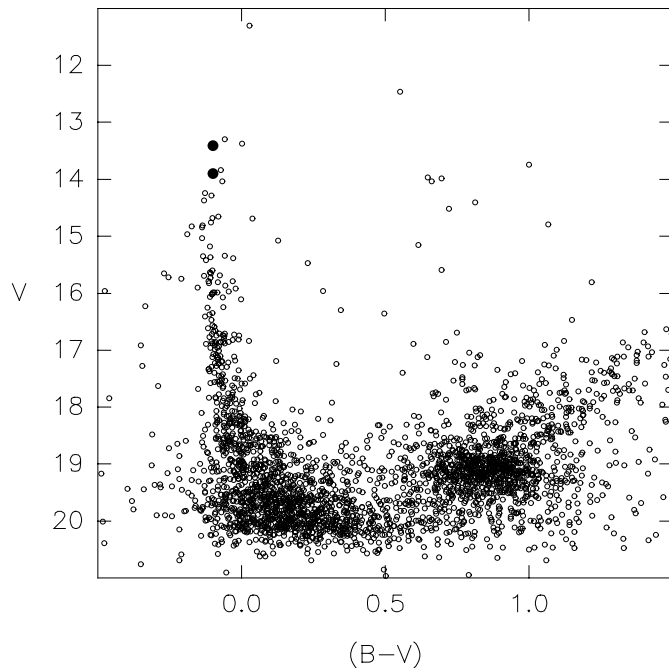


**Fig. 4.** Color-Magnitude diagram for the field surrounding HV 2543. The two filled circles represent the magnitude estimates for the components of HV 2543. Magnitudes and colours are not corrected for extinction.

In this figure, the presence of an OB association covering the whole frame ( $9'$  of diameter) is evident. Ostrov et al. (1999) found evidence of a stellar association surrounding the massive binary system Sk-67°105. The relatively small angular distance between the two stellar groups ( $\sim 9.5'$ ) suggests that they are probably related.

We have obtained spectroscopic data for five stars in the neighbourhood of Sk-67°105. For these stars, we have estimated the reddening by comparison between the intrinsic  $(B - V)_0$  colours given by Schmidt-Kaler (1982) and FitzGerald (1970) and the observed colours. We derived  $E(B - V) = 0.17 \pm 0.015$ , while for HV 2543 itself we obtained  $E(B - V) = 0.20$ . A detailed study of these OB associations will be presented in a forthcoming paper.

## 4. Discussion

We note that the radius derived for the O8 component is substantially larger than the one obtained by Niemela & Bassino (1994). In fact, the spectroscopic data suggest that the luminosity of the O9 star is larger than that of the O8 star, which caused Niemela & Bassino to refer to the O9 component as “primary”, even though it is the one presenting the largest radial velocity amplitude, and consequently the less massive component of the binary system. Hence, we explored alternative solutions to the light curve that could yield a smaller radius for the O8 component. The values  $R_1 \sim 12.75$ ,  $R_2 \sim 15.31$ ,  $M_1 \sim 21.91$  and  $M_2 \sim 19.34$ , in solar units, provide a good fit to the light curve, although they require a value of  $q$  near 0.9, which is not compatible with the radial velocity data. Hence we have discarded this

solution, which on the other hand, implies a rather low value of the distance modulus, namely 18.18, assuming  $A_V = 0.62$  (see below) and adopting the temperature scale of Chlebowski & Garmany (1991). This value would result even smaller if a lower temperature scale is adopted.

On the other hand, the temperature difference between the two components of HV 2543 resulting from the light curve analysis is larger than that suggested by the corresponding spectral types. This fact might be due to the difference between the spectral features of the unperturbed back sides and the heated inner sides of the stars. Also should we have in mind that the mass transfer history of the system might account for significant departures of the He abundances relative to those regarded as normal for LMC members, and this effect could influence some spectral lines of the secondary component.

To solve these puzzles, high dispersion spectroscopy would be desirable.

The semimajor axis and star dimensions of this system are alike those determined by Pritchard et al. (1998) for HV 2241, but the masses are somewhat smaller. We presume that these systems have experienced case A mass transfer, being now in the slow stage of mass exchange. In these cases, the mass gainer should be indistinguishable of a normal star, excepting that it would stand on an isochrone corresponding to a shorter age (see Vanbeveren et al. 1998). From the stellar models of Schaerer et al. (1993) (for single stars) we found that a  $25M_{\odot}$  star takes  $\sim 6.7$  Myr until its radius grows to  $15R_{\odot}$ , but such star would have an effective temperature of only 30000 K. The radius and effective temperature derived for the O8 star are consistent with those of a single star of some 3.7 Myrs and  $\sim 40M_{\odot}$ , completely out of the range of masses compatible with the radial velocity data. We note that a similar problem arises from the analysis of AB Crucis (Lorenz et al. 1994).

It is clear that there are a series of phenomena that we do not fully understand, and consequently, our analysis can not be considered definitive. The errors given for the derived parameters must be considered with caution. True errors are not easy to estimate analytically, since they depend on the importance of phenomena that are not properly accounted for, such as wind shocks, uncertainty of the adopted temperature scale, radiation pressure effects, etc. In fact, the sizes and positions of the spots used to model empirically the O'Connell effect are rather arbitrary, and an equally satisfactory solution could be found with other parameters, but these details do not affect meaningfully the derived star dimensions.

From our photometry we determine  $(B - V) = -0.11 \pm 0.015$  for HV 2543. This value is somewhat redder than  $-0.18$ , obtained by Isserstedt (1979). However, given that Isserstedt does not detect the variability of HV 2543, we think that both measures are still in reasonable agreement. If we assume a  $(B - V)_0$  of  $-0.31$  (Schmidt-Kaler 1982),  $R = 3.1$  (Koornneef 1982) then it results an  $A_V = 0.62$  for HV 2543. This value does not depend on which temperature scale we adopt, since for the range of temperatures of the O-type stars the  $(B - V)$  colours are degenerated.

Estimating the bolometric corrections according to Massey & Hunter (1998), we derive a distance modulus of  $(m - M)_0 = 18.31 \pm 0.2$  to  $18.40 \pm 0.2$ , depending on the adopted temperature scale. The error accounts for the uncertainties in the estimates of  $R$  and the bolometric corrections. This distance modulus must be considered with caution, since this system has experienced strong mass transfer and exhibits the above mentioned anomalies.

## 5. Conclusions

We have presented a CCD  $V$  light curve of the eclipsing binary HV 2543 (Sk-67°117) in the LMC. The light curve appearance is almost symmetric, with a slight ( $\sim 0.02$  V magnitudes) O'Connell effect. From  $BV$  photometry of the surrounding field, we found that HV 2543 probably belongs to an OB association not previously identified.

We have analysed this light curve and the published radial velocity data using the Wilson-Devinney code, finding that HV 2543 is a semidetached system with the less massive and less luminous member filling its Roche lobe. The primary minimum occurs when the O8 component is behind the O9. From our analysis, we derived fundamental parameters for this system, obtaining  $M_1 = 25.63 \pm 0.7$ ,  $M_2 = 15.63 \pm 1.0$ ,  $R_1 = 15.54 \pm 0.4$  and  $R_2 = 13.99 \pm 0.4$  in solar units. Some discrepancies between the present results and those derived from the previous spectroscopic analysis (Niemela & Bassino 1994), should be thoroughly addressed in future works.

We found that this system has experienced significant mass exchange, being the present most massive star the originally less massive.

*Acknowledgements.* The authors acknowledge use at CASLEO of the CCD and data acquisition system supported under U.S. National Science Foundation grant AST-90-15827 to R. M. Rich. The focal reducer in use at CASLEO was kindly provided by Dr. M. Shara. This research has made use of the Astronomical Data Center catalogs. We are indebted to the staff of CASLEO for valuable help during the observing runs. We are grateful to V.S. Niemela for her vigorous comments made during the preparation of this paper. We would also like to thank to the referee for the suggestions that allowed to improve the presentation of the paper.

## References

- Chlebowski T., Garmany C.D., 1991, ApJ 368, 241
- Davidge T.J., Milone E.F., 1984, ApJS 55, 571
- FitzGerald M.P., 1970, A&A 4, 234
- Gaposhkin S., 1970, Smithsonian Ast. Obs. Spec. Rep. 310 277
- Isserstedt J., 1979, A&AS 38, 239
- Koornneef J., 1982, A&A 107, 247
- Landolt A.U., 1992, AJ 104, 340
- Leung K.C., Wilson R.E., 1977, ApJ 211, 853
- Lorenz R., Mayer P., Drechsel H., 1994, A&A 191, 185
- Lucy L.B., 1976, ApJ 205, 208
- Massey P., Hunter D.A., 1998, ApJ 493, 180
- Minniti D., Clariá J.J., Gómez M.N., 1989, Ap&SS 158, 9
- Niemela V.S., Bassino L.P., 1994, ApJ 437, 332

- Ostrov P.G., Niemela V.S., Morrell N.I., 1999, In: Chu Y.-H., Suntzeff N.B., Hesser J.E., Bohlender D. (eds.) IAU Symp. 190, New Views of the Magellanic Clouds. ASP Conf. Series, in press
- Payne-Gaposchkin C.H., 1971, Smithsonian Contr. to Astrophysics No. 13
- Pritchard J.D., Tobin W., Clark M., Guinan E.F., 1998, MNRAS 297, 278
- Rucinski S.M., 1969, Acta Astron. 19, 245
- Sanduleak N. 1969, Cerro Tololo Inter-American Obs. Contr. No. 89
- Schaerer D., Meynet G., Maeder A., Schaller G., 1993, A&AS 98, 523
- Schmidt-Kaler Th., 1982, In: Shaifers K., Voigt H.H. (eds.) Landolt-Börnstein, New Series, Group VI, Vol. 2/b
- Smith Neubig M.M., Bruhweiler F.C., 1999, AJ 117, 2856
- Stetson P.B., 1987, PASP 99, 191
- Stetson P.B., 1991, In: Grosbøl P.J., Warmels R.H. (eds.) 3rd ESO/ST-ECF Data Analysis Workshop, p. 187
- Vanbeveren D., De Loore C., Van Rensbergen W., 1998, A&AR 9, 63
- van Hamme W., 1993, AJ 106, 2096
- Wilson R.E., 1990, ApJ 356, 613
- Wilson R.E., Devinney E.J., 1971, ApJ 166, 605